

The Topological Non-connectivity Threshold in anisotropic long-range interacting spin systems

F. Borgonovi,^{1,2} G. L. Celardo,¹ and R. Trasarti-Battistoni¹

¹*Dipartimento di Matematica e Fisica, Università Cattolica, via Musei 41, 25121 Brescia, Italy*

²*I.N.F.N., Sezione di Pavia, Italy*

(Dated: November 3, 2019)

Classical and quantum characteristics of the Topological Non-connectivity Threshold (TNT), introduced in F.Borgonovi, G.L.Celardo, M.Maianti, E.Pedersoli, *J. Stat. Phys.*, 116, 516 (2004), have been analyzed from the dynamical point of view. A quantum analogue of the classical TNT is given, in term of spectral and dynamical properties, even if, due to quantum tunneling a proper definition is necessary. This opens new interesting perspectives in term of the possibility to study the intriguing quantum-classical transition through Macroscopic Quantum Tunneling.

PACS numbers: 05.45.-a, 05.445.Pq, 75.10.Hk

I. INTRODUCTION

The magnetic properties of materials are usually described in the frame of system models, such as Heisenberg or Ising models where rigorous results, or suitable mean field approximations are available in the thermodynamical limit. On the other side, modern applications require to deal with nano-sized magnetic materials, whose intrinsic features lead, from one side to the emergence of quantum phenomena[2], and to the other to the question of applicability of statistical mechanics. Indeed, few particle systems do not usually fit in the class of systems where the powerful tools of statistical mechanics can be applied at glance. In particular, an exhaustive theory able to fill the gap between the description of 2 and 10^{23} interacting particles is still missing. Moreover, also important well-established thermodynamical concepts as the temperature, become questionable at the nano-scale[3].

In a similar way, long-range interacting systems belong, since long, in the class where standard statistical mechanics cannot be applied *tout court*. Indeed, they display a number of bizarre behaviors, to quote but a few, ensemble inequivalence[4], negative specific heat, temperature jumps and long-time relaxation (quasi-stationary states)[5]. Therefore, from this point of view, few-body short-range interacting systems share some similarities with many-body long-range ones.

Within such a scenario, and thanks to the modern computer capabilities, it is quite natural take a different point of view, starting investigations directly from the dynamics, classical and quantum as well.

It was in this spirit that, few years ago, a topological non-connection of the phase space was discovered[1] in a class of anisotropic spin systems. This was initially called, for historical reasons[6], breaking of ergodicity, meaning with that a trivial consequence, namely that the system can not be ergodic (the phase space is exactly decomposable in two unconnected parts)[7], even if we prefer here to call it Topological Non-connectivity Threshold (TNT).

This result, was found first numerically and later ana-

lytically, in a class of models, the anisotropic Heisenberg models, where important and rigorous results have been obtained during the last century, in the thermodynamical limit only. Nevertheless, to the best of our knowledge, apparently nobody took care of the dynamics and, consequently, of this simple but relevant property.

This dynamical point of view has few interesting classical consequences. First of all it explains, from the point of view of microscopic dynamics, the possibility of ferromagnetic behavior in small system. Indeed, in absence of external field and external noise (temperature) a magnetized system, (belonging to one branch of the non-connected phase space) remains magnetized simply because it cannot move to the other one.

It is worth of mention the recent results[8] about topological phase transitions, surely related to the Topological Non-connectivity Threshold, even if they are still concerning the thermodynamical limit only.

We therefore begin with a short introduction about the topological properties of the disconnection border, for finite and infinite systems in Section II. In particular we would like to answer the following question: what happen to TNT and to the related spin configuration when the number of particles grows? It is exactly answering this question that the deep connection between TNT and long-range interaction comes out. Our results[9], can be summarized as follows:

1) For finite sized systems TNT exists for short range and long range as well, as soon as anisotropy persists.

2) When the number of particles becomes large the energy size of the non-connected region goes to zero with respect to the total energy size for short range interaction while it goes to some finite quantity for long range ones.

In Section III we switch to the dynamical properties first found in [10] accomplishing such transition and the relations with ordinary phase transitions, using modern tools as the large deviation techniques [11] within the microcanonical formalism.

Quantum effects in such small magnetic systems can not be neglected, in principle, even if the usual viewpoint [2] is to consider magnetic domains as quantum

objects with huge spin number. Here we take a different approach, and similarly to the classical case we use the microscopic dynamics in order to describe the system behavior. This we do in order to describe, at the beginning in a pedagogical way, how TNT looks like in the quantum world and how its features reflect on the quantum dynamics[12].

On the other side what we have in mind now and in our future plans, is to show its relevance with respect to the complicated transition between the classical and quantum world. For instance, it is well known that quantum particles can tunnel across potential barriers at variance with the classical ones. What is less obvious is that a macroscopic variable, such as the magnetization, can do the same. This phenomenon, known as Macroscopic Quantum Tunneling, well described in [2] is an important step in the so-called Leggett program [13] for a better comprehension of the classical-quantum transition. Thus, in Section IV we describe the TNT from a quantum point of view, and how the semiclassical limit is recovered. Last, we show the relevance of TNT in single-spin models used in micromagnetism, featuring the TNT as a perturbative threshold.

II. ENERGY AND TOPOLOGY IN CONFIGURATION SPACE

As a paradigmatic example of TNT, let us consider the following class of lattice spin models, described by the Heisenberg-like Hamiltonian:

$$H = \frac{\eta}{2} \sum_{i \neq j}^N \frac{S_i^x S_j^x}{r_{ij}^\alpha} - \frac{1}{2} \sum_{i \neq j}^N \frac{S_i^y S_j^y}{r_{ij}^\alpha} \quad (1)$$

where S_i^x, S_i^y, S_i^z are the spin components, assumed to vary continuously; $i, j = 1, \dots, N$ label the spins positions on a suitable lattice of spatial dimension d , and r_{ij} is the inter-spin spatial separation therein. Here for simplicity we consider a $d = 1$ lattice. (See [9] for extensions to $d = 2, 3$.) For later notational convenience, we define the single-spin vector $\vec{S} = (S_i^x, S_i^y, S_i^z)$ and the N -spin configuration $\vec{S}^N = (\vec{S}_1, \vec{S}_2, \dots, \vec{S}_N)$. The tip of each i -th spin is taken to lie on the unit sphere, i.e. it satisfies the constraint $(S_i^x)^2 + (S_i^y)^2 + (S_i^z)^2 = 1$. Also, $\alpha > 0$ parametrizes the range of interactions (decreasing range for increasing α) and $0 < \eta < 1$ parametrizes the XY anisotropy.

For $\alpha = \infty$ we recover nearest-neighbor interactions, while $\alpha = 0$ corresponds to infinite-range interactions.

A mean-field model is obtained by setting $\alpha = 0$ and including as well the self-interaction pairs $i = j$:

$$H_{mf} = \frac{\eta}{2} N^2 (m_x)^2 - \frac{1}{2} N^2 (m_y)^2, \quad (2)$$

where $m_{x,y,z} = (1/N) \sum_i^N S_i^{x,y,z}$. While this might be thought of as a negligible modification for $N \rightarrow \infty$, nevertheless it has non-negligible effects concerning the chaoticity properties of the system. Indeed, the dynamics of the truly mean-field $\alpha = 0$ system turns out to be exactly integrable[10].

Here we are not interested in the most general spin Hamiltonian giving rise to a TNT (for instance in [1, 10] a term containing a transversal magnetic field B_z has been added to H). Rather, we focus on the very simple Hamiltonian (1) which already contains the two essential ingredients which give rise to the TNT, i.e. anisotropy and long-range. Let us therefore spend a few words about the physical motivations leading to the the introduction of anisotropy and long-range.

Needless to say, in real magnetic systems, anisotropy is by far more common than isotropy. From the theoretical point of view, it can be shown[14, 15] that magnetocrystalline anisotropy is connected via orbital and spin-orbit interaction to the atomic structure of a magnetic material. Moreover, there is the possibility of enhancing the magnetic anisotropy by artificially decreasing the dimension as in 1D wires or 2D thin films on a substrate[16, 17, 18, 19, 20, 21, 22]. That way, magnetic anisotropy per atoms can be increased by a factor up to 10^3 with respect to the bulk properties, see [23, 24, 25] for theoretical calculations. Here we do not want to describe all kind of possible anisotropies; we simply encapsulate the problem of anisotropy inside one single and easy-to-handle parameter η , in order to simplify the study of the minimum-energy configurations later on.

Despite its somewhat artificial character, the introduction of long-range as parametrized by α requires some considerations too. On one hand, magnetic interactions due to the quantum exchange mechanism are usually short-ranged, so that a parametrization in term of nearest-neighbor coupling ($\alpha = \infty$) well describes the physics. On the other hand other magnetic interactions such as the dipole-dipole ($\alpha = 3$) or the interaction with the electron spin of the conduction band of a metallic substrate (RKKY interaction [26]) require more complicated functions of the interspin distance. Here we do not want to describe all kind of known and unknown possible interactions; we simply model the problem of the range of interaction with one single parameter (α), in order to simplify the study of the $N \rightarrow \infty$ limit. But let us first turn to topology and introduce some useful definitions.

Depending on the specific N -spin configuration the corresponding energy $E = H(\vec{S}^N)$ will vary according to (1).

One, not necessarily unique, configuration \vec{S}_{min}^N , to be specified soon, turns out to have minimum energy E_{min} , defined by the minimum of the Hamiltonian (1) over all conceivable configurations:

$$E_{min} = \text{Min} [H] . \quad (3)$$

Since $0 < \eta < 1$ the minimum energy configuration \vec{S}_{min}^N

is attained when all spins are aligned along the Y axis, which defines implicitly the easy axis of magnetization.

In the same way, let us define the TNT energy E_{tnt} as the minimum energy compatible with the constraint of zero magnetization along the easy axis of magnetization:

$$E_{tnt} = \text{Min} [H \mid m_y = 0]. \quad (4)$$

corresponding to some other N -spin configuration \vec{S}_{tnt}^N to be specified later.

By definition, it is $E_{tnt} \geq E_{min}$, and in particular it may happen that $E_{tnt} \neq E_{min}$. This situation is what we call topological non-connection, and its physical (dynamical as well as statistical) consequences are rather interesting. Indeed, suppose to have a system with initially a definite sign of magnetization, say $m_y > 0$ (ferromagnetic sample) and an energy value $E_{min} \leq E \leq E_{tnt}$. During its dynamics, the system evolves upon the constant energy surface $H(\vec{S}^N) = E$ in configuration space. Nevertheless, due to the continuity of the equations of motion the magnetization $m_y(t)$ may change size (it is not a constant of motion) but it can never assume a negative value. Indeed, in order to change its sign, it should have to cross the $m_y = 0$ plane, which instead does not belong to the $H = E$ surface. In other words this means that the energy surface is topologically non-connected in two parts each characterized by a definite sign of magnetization $m_y < 0$ or $m_y > 0$, and no dynamical path is possible between them: de-magnetization is in principle impossible for E below E_{tnt} . Of course, the application of a magnetic field, or a thermal noise, can give the energy necessary to overcome the energy barrier, thus in principle - if not in practice - allowing for a magnetic reversal.

On the contrary, for energy values $E > E_{tnt}$, de-magnetization is in principle possible, and we may speak in some sense of a paramagnetic sample. Even if in principle dynamically possible, this does not mean that, for any combination of parameter values, a magnetized sample can actually de-magnetize within a given finite time. As reported in [10] some invariant multidimensional structures can appear in phase-space preventing the motion from covering the whole energy surface. This lack of ergodicity is well known in 2D Hamiltonian systems, where KAM tori prevent motion from wandering the whole phase space [27], while it turns out to be more complicated in multidimensional system, see for instance the famous Fermi-Pasta-Ulam problem (for interesting reviews see [28, 29]). Such invariant structures usually disappear in presence of strongly chaotic motions [27]. We can therefore say that strong chaos is somehow another necessary ingredient in order to have a paramagnetic sample.

While for finite N systems the anisotropy is the only necessary ingredient in order to have a TNT, the picture changes radically when the limit $N \rightarrow \infty$ is taken. Indeed, in such a case it is physically more relevant to look whether the non-connected region of energy values

remains a significant fraction of the whole energy region (the minimum energy goes to infinity when N goes to infinity). To this end it will be useful to look for the following non-connection ratio:

$$r = \frac{E_{tnt} - E_{min}}{|E_{min}|}, \quad (5)$$

where in the denominator E_{min} has been taken (instead of the whole energy range), since, in such kind of models, one is usually interested in the negative energy range only.

This allows to define a disconnected system if $r \rightarrow \text{const} \neq 0$, in the limit $N \rightarrow \infty$. Here below we will see why and how this whole comes by in our models, concentrating on the Topology of spin configuration space as a function of energy E at given magnetization $m_y = 0$.

The minimum-energy configuration \vec{S}_{min}^N (all spins aligned along the Y -axis), can also be thought of as composed of 2 equal blocks of $N/2$ spins, all up. Correspondingly, the minimum energy $E_{min} < 0$ can be split into 3 contributions, namely 2 equal intra-block bulk energies $E_{\uparrow} < 0$ plus 1 inter-block interaction energy $V_{\uparrow\uparrow} < 0$. Flipping just 1 block, its bulk energy does not change, i.e. $E_{\uparrow} = E_{\downarrow} < 0$, but the interaction energy reverses sign to $V_{\uparrow\downarrow} = -V_{\uparrow\uparrow} > 0$. However, in such a new configuration $\vec{S}_{\uparrow\downarrow}^N$ the magnetization is now $m_y = 0$. Both bulk energies are as low as they can, while the constraint $m_y = 0$ frustrates the total energy to rise above E_{min} by an amount $2|V_{\uparrow\uparrow}|$. We therefore take $E_{\uparrow\downarrow} = E_{min} + 2|V_{\uparrow\uparrow}|$ as a somewhat obvious candidate for E_{tnt} and the related spin configuration $\vec{S}_{\uparrow\downarrow}^N$ as the TNT spin configuration \vec{S}_{tnt}^N .

Extensive numerical simulations using constrained optimization and analytical estimates as well[9], have indicated that, even if $\vec{S}_{\uparrow\downarrow}^N$ is not, rigorously speaking, the TNT spin configuration, it can be considered a good first approximation. While this is somehow obvious for short range interacting systems, it cannot be rigorously true for any small α . Indeed, for $\alpha \rightarrow 0$, $E_{\uparrow\downarrow}$ becomes a positive quantity while, for instance, a configuration with all spins aligned along the X axis (thus having $m_y = 0$), with alternating signs has lower (negative) energy.

Quite generally, the problem of finding the TNT configuration for any finite N , α and η can be solved only numerically. Nevertheless, concerning the large N limit it is possible to make a few definite statements.

First of all it is possible to show that, for any $\alpha \neq 0$ a sufficiently large N_α exists such that for $N > N_\alpha$ the TNT spin configuration is close to $\vec{S}_{\uparrow\downarrow}^N$. With close we mean that $E_{tnt} - E_{\uparrow\downarrow}$ is a finite quantity independent of N .

An example of the TNT spin configuration is given in Fig. 1. As one can see, excluding a small central domain, the spins are arranged in two blocks with opposite spins.

Last but not least, concerning the disconnection ratio,

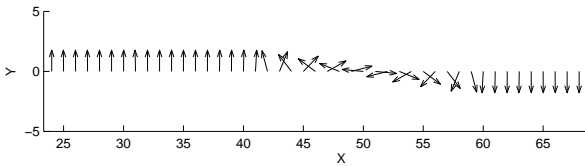


FIG. 1: TNT spin configuration. Here is $\alpha = 0.1$, $N = \eta = 0.9$. Only the central part of the chain has been shown.

it is relatively easy to show[9] that:

$$\lim_{N \rightarrow \infty} r = \begin{cases} 2 - 2^\alpha & \text{for } \alpha < 1 \\ 0 & \text{for } \alpha \geq 1. \end{cases}$$

so that a disconnected system can have a significant disconnected range only in the long-range case.

Let us finally remark that, in any case, either at or infinite N and for long- or short-range, $E_{tnt} \neq$ for anisotropic interactions.

III. DYNAMICS AND THERMO-STATISTICS: CLASSICAL

Here, we show how to impose a self-consistent Hamiltonian dynamical evolution upon the spin systems described by (1). Afterward, we will employ such dynamical equations, numerically integrated for long enough times, to study the time-evolution of $m_y(t)$.

For each i the spin components S_i^x, S_i^y, S_i^z satisfy the usual commutation rules for angular momenta, i.e. $\{S_i^x, S_j^y\} = \delta_{ij} S_i^z$, (and cyclic) where $\{, \}$ are the canonical Poisson brackets. As usual, (and this procedure immediately translates to the quantum case [12]), we derive the dynamical equations directly from the Hamiltonian (1) as:

$$\begin{aligned} \frac{dS_i^x}{dt} &= \{H, S_i^x\} \\ \frac{dS_i^y}{dt} &= \{H, S_i^y\} \\ \frac{dS_i^z}{dt} &= \{H, S_i^z\} \end{aligned} \quad (7)$$

As is well-known, for such dynamical equations the total energy E and the spin moduli $|\vec{S}_i|^2 = 1$ are constants of the motion.

The dynamics is usually characterized[1], for energies E not too close to E_{min} by chaotic motion (as given by a positive Lyapunov exponent). Here we focus mostly on the dynamical evolution of the magnetization.

As a start, following [9, 10] we look at the instantaneous magnetization $m_y(t)$ started with some E and $m_y(0)$ and evolved according to (7). Typical examples of evolution curves of $m_y(t)$, for different energy values, are shown in Fig. 2.

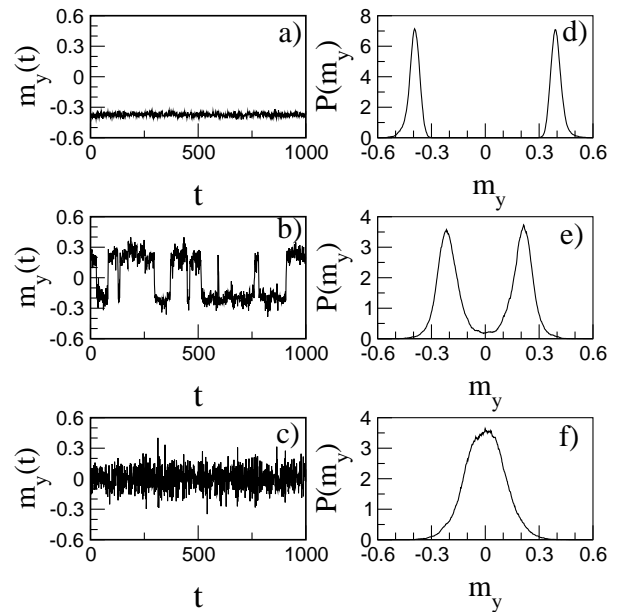


FIG. 2: Left column (a,b,c) : time evolution of the magnetization $m_y(t)$ for different specific energy values. Right column (d,e,f) : probability distribution of the magnetization at a given specific energy. Parameters are $\alpha = 0$, $\eta = 1$, $N = 10$. Upper line ((a,d) below the TNT) : $E/N = -0.7$. Middle line ((b,e) between the TNT and the statistical thresholds $E/N = -0.3$). Lower line ((c,f) above the statistical threshold) $E/N = 0.1$.

As explained previously, the magnetization reversal is related to the structure of the phase space. In the same Fig. 2 the dynamics of magnetization (left column) is accomplished by the probability distribution of m_y : $P(m_y)$ as taken by a random sampling on the energy surface $H = E$.

As one can see, for $E < E_{tnt}$ (Fig. 2d) the two peaks of the distribution are well separated, while for $E > E_{tnt}$ (Fig. 2e) they come close. At some energy value, that we call E_{stat} one single peak in the probability distribution appears (Fig. 2f). Since probability distribution is a measure of the density of states, i.e. of the entropy, one can expect the presence of a phase transition at E_{stat} .

As for the dynamical behavior of the magnetization, let us only remark that, while the cases (a) and (c) in Fig. 2 are self-explanatory, few comments are in order regarding (b). One can define a jumping time, from the time necessary to magnetization to reverse its sign. In presence of strong chaos (dependent on the parameters N and E) reversals occur erratically and the distribution of jumping times follows a Poisson distribution. Any deviation from such distribution, for large N and large negative E values, signals the presence of invariant curves preventing the motion to switch from one peak to the other one.

Remarkably, and somewhat reminiscent of a critical phase transition, reversal times diverge at the critical energy E_{tnt} as a power law of E , as shown in Fig. 3:

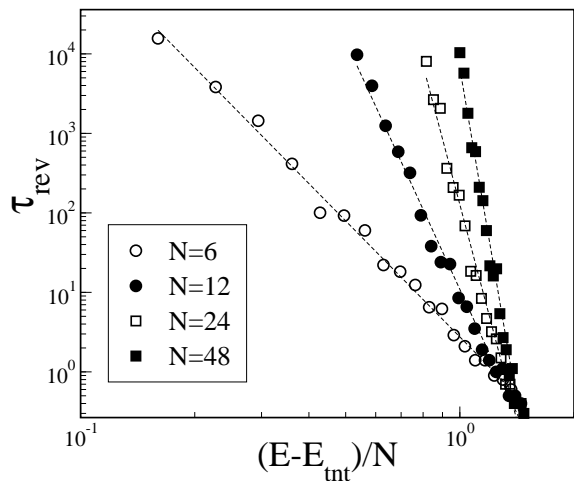


FIG. 3: Divergence of magnetization reversal times close to the TNT. Here is $\alpha = 0$, $\eta = 1$, and different N values as indicated in the insert. Lines are the best fit according to Eq. (8).

$$\tau_{rev} \sim \left[\frac{E - E_{tnt}}{N} \right]^{-\gamma(N)} \quad (8)$$

where $\gamma(N) \propto N$. Remarkably, such a behavior can be qualitatively - and almost quantitatively - explained by statistical considerations. Before that, let us remark that (8) can be inverted for E at any fixed N , thus giving a τ -depending characteristic energy $E_{rev}(\tau)$. We will see the physical meaning of E_{rev} in a while; here we just note that, since (8) holds only for $E > E_{tnt}$, it will also be $E_{rev} > E_{tnt}$.

A detailed statistical analysis, can be performed on the mean field Hamiltonian (2), and both E_{stat} and E_{tnt} can be computed analytically from the microcanonical (i.e., state-counting entropy) $S(m_y, \epsilon)$ using techniques from large deviations theory (see [10] for details).

Given $S(m_y, \epsilon)$ we may then use it to define the thermo-statistical probability distribution as usual: $P_{stat}(m_y, \epsilon) = \exp[S(m_y, \epsilon)]$. In principle, this gives us all we were looking for. For $N \rightarrow \infty$ [10] a second order phase transition occurs at E_{stat} . It is thus natural to put the following question: does $E_{tnt} \rightarrow E_{stat}$ for $N \rightarrow \infty$? Or, in other words, at what energy a physical system will make the transition?

As for the first question, the answer is trivial, since it is possible to get a closed expression for both E_{tnt} and E_{stat} [1, 10]: the two limits stay separate when $N \rightarrow \infty$. So, at what energy will the system make a transition, from a “ferromagnetic-like” state to a “paramagnetic-like” one? The answer depends on what quantity we are looking for.

Adopting, a viewpoint as close as possible to the experimental one, we have to introduce an observational time t_{obs} , during which the experiment can be performed

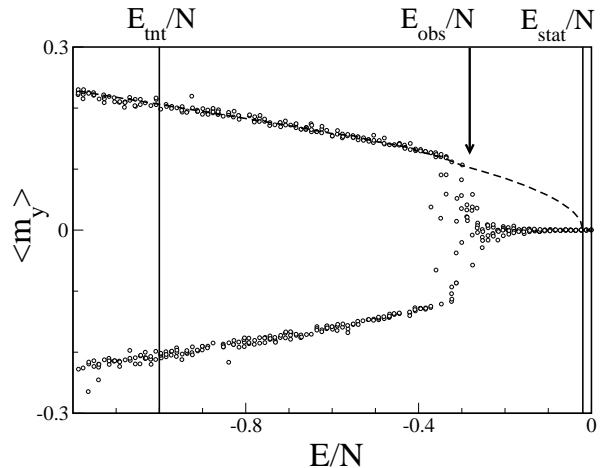


FIG. 4: Average (dynamical) magnetization as a function of the specific energy (circles). Dashed line has been obtained analytically from the mean field model (2). Here is $N = 60$, $\alpha = 0$, $\eta = 1$. For the sake of comparison the statistical and the topological non-connectivity thresholds have been indicated as vertical lines. Also indicated, as a vertical arrow, the expected energy threshold.

and since the time average is usually the measured value, let us introduce

$$\langle m_y(t) \rangle = \int_0^{t_{obs}} dt m_y(t). \quad (9)$$

This quantity as a function of the energy E can be compared with $m_y^{stat}(E)$, obtained from the most likely values of $P_{stat}(m_y, E)$ (the maxima of the distribution).

The comparison is shown in Fig. 4, where we have also indicated, as vertical lines the thresholds E_{stat} and E_{tnt} .

Of course, below E_{tnt} and above E_{stat} the two averages coincide, at variance with the region between them. Also, the effective transition, if given by $\langle m_y \rangle$, occurs at some intermediate energy, different from both E_{tnt} and E_{stat} . This is not surprising, since E_{tnt} and E_{stat} refers both at some limiting properties, the former for any finite N system when the average time $t \rightarrow \infty$, the latter at any time when $N \rightarrow \infty$.

It is interesting to note, that, inverting Eq. (8) at the observation time t_{obs} one gets $E_{rev}(t_{obs})$ which is in fairly good agreement with the observed transition energy, see Fig. 4.

IV. THE QUANTUM TOPOLOGICAL NON-CONNECTIVITY THRESHOLD

The results found in the classical model guided our investigations on the quantum side. We are mainly interested here in the quantum signature of the classical TNT, and on its relevance with respect to the quantum reversal time of the magnetic moment, in the semiclassical limit. For this reason we will consider here a very

simple example for which we can analytically compute the TNT, classically.

We consider a system of N particles of spin l , described by the same Hamiltonian (1) considered in the classical case with $\alpha = 0$, so we have:

$$\hat{H} = \frac{\eta}{2} \sum_{i=1}^N \sum_{j \neq i} \hat{S}_i^x \hat{S}_j^x - \frac{1}{2} \sum_{i=1}^N \sum_{j \neq i} \hat{S}_i^y \hat{S}_j^y, \quad (10)$$

where $0 < \eta \leq 1$ is the anisotropy constant. Quantization of the Hamiltonian follows the standard rules. According to the correspondence principle, the classical limit is recovered as $l \rightarrow \infty$. As in the classical case we fix the modulus of the spins to one. This can be achieved with an appropriate rescaling of the Planck constant, $\hbar \rightarrow \hbar/|S_i| = 1/\sqrt{l(l+1)}$. With this choice, in the classical limit, $l \rightarrow \infty$ ($\hbar \rightarrow 0$), the spin modulus remains equal to 1. Because of the infinite range nature of the interaction, the Hamiltonian (10) is a completely symmetric operator with respect to particle exchange. It is thus natural to limit ourselves to subspaces of definite symmetry. Specifically, we consider the bosonic case (an ensemble of integer spins), so we will limit our analysis in the subspace of all possible completely symmetric states, with dimension $\mathcal{N} = (N+2l)!/(N!(2l)!)$. This choice reduces considerably the dimension of the Hilbert space, allowing to extend our analysis further in the classical limit. An important property of the Hamiltonian (10) is its invariance under a π rotation about the z -axis: the Hamiltonian commutes with the operator $\exp(i\pi \sum \hat{S}_i^z)$ and its eigenstates can be labeled as odd (-) or even (+) according to whether they change or do not change sign under such rotation.

We first analyze the spectral properties and we establish the existence of a quantum disconnection threshold in close correspondence with the classical one. An analytical estimate of this quantum threshold is given. We will then study the system from a dynamical point of view, analyzing the time scale for quantum magnetic reversal and comparing the quantum magnetic reversal times with the classical ones. Finally we will consider some simple phenomenological models used in micromagnetism, showing how the TNT can be considered a perturbative threshold.

A. Semiclassical limit

Numerical diagonalization of (10) gives rise to a quasi-degenerate energy spectrum with a energy splitting increasing with the energy. In the low energy region the spectrum is organized in quasi degenerate doublets, constituted by an even and an odd eigenstate, E_+^i and E_-^i , separated by an energy difference $\delta_i = |E_+^i - E_-^i|$. It is also useful to define the spacing between eigenstates of the same parity as $\Delta_i = |E_+^{i+1} - E_+^i|$. Note that the doublets are well defined only when $\delta_i \ll \Delta_i$.

The energy difference $\delta(E)$ depends exponentially on the energy E for $\delta \leq \Delta$. This allows to identify, at least numerically, a possible quantum analogue of the classical TNT as the energy E^* at which

$$\delta(E^*) \simeq \Delta(E^*)$$

An analytical expression of the TNT can also be given if we think of E^* as a quantum correction to the classical TNT. Indeed, since in the classical case, E_{tnt} had been obtained computing the minimum[1] of $-(\eta/2) \sum (S_i^x)^2$ (for $\eta > 0$), we may assume that the lowest eigenvalues of the same operators could give an analytical estimate of the quantum threshold:

$$\begin{aligned} E_{tnt}^q &\sim -\frac{N\eta}{2}(\hbar l)^2 \text{ for } \eta > 0 \\ E_{tnt}^q &\sim \frac{N\eta}{2}(N-1)(\hbar l)^2 \text{ for } \eta < 0. \end{aligned} \quad (11)$$

The numerical values E^* and our analytical estimate E_{tnt}^q are in fair agreement and they both converge to E_{tnt} in the semiclassical limit $l \rightarrow \infty$ [12].

Let us now analyze the time scale for magnetic reversal in the quantum system, comparing the results with the classical ones[10]. Since in the classical case the reversal times have been determined at a fixed energy (micro-canonical approach), we adopt here the same procedure and compute the reversal time of the quantum average magnetization starting from an ensemble of initial states, $|\psi\rangle$, obtained choosing randomly energy eigenstates in a narrow energy interval: $|\psi\rangle = \sum_E^{E+\Delta E} C_E |E\rangle$. The coefficients C_E have been randomly chosen in modulus and phase and such that $\sum_E^{E+\Delta E} |C_E|^2 = 1$. Since the total magnetization along the easy-axis, \hat{m}_y , connects only energy eigenstates with different parity, we have:

$$\langle m_y(t) \rangle = 2\mathcal{R}e \left\{ \sum_{E_+, E_- = E}^{E+\Delta E} C_{E_+}^* C_{E_-} e^{-it(E_- - E_+)/\hbar} m_y^\pm \right\}, \quad (12)$$

where m_y^\pm are the matrix elements of \hat{m}_y between the states $|E_\pm\rangle$. From $\langle m_y(t) \rangle$ we compute the time of first passage through zero for each initial state of the ensemble. From these times we obtain the average magnetic reversal time τ . Before presenting the results of our analysis let us notice that in the quantum case, at variance with the classical one, we are legitimate to ask what is the time scale for magnetic reversal in the whole energy range. Indeed, since the energy spectrum is non-degenerate, the average magnetization will soon or later reverse its sign, even below the TNT. This effect can be interpreted as a manifestation of Macroscopic Quantum Tunneling [2] since the total magnetization can be a macroscopic quantity.

Above the classical TNT, see Fig. 5, the quantum times agrees with the classical ones at high energy values while they are smaller near the classical TNT. This is not surprising since the possibility of tunneling will enhance the

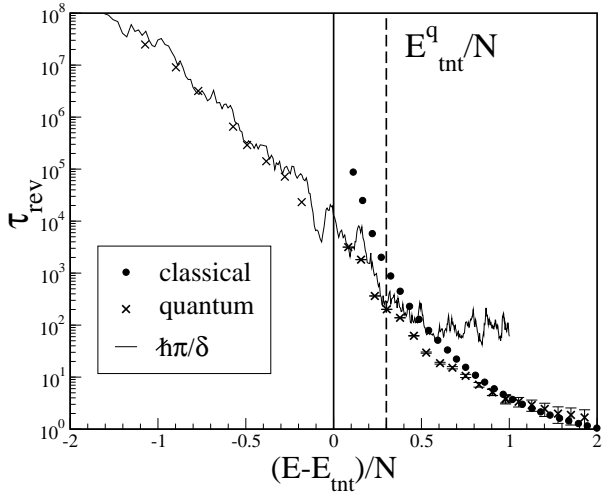


FIG. 5: Quantum average reversal times, τ_{rev} (crosses), as a function of the shifted specific energy is shown for the case $N = 6$, $\eta = 1$ and $l = 4$, and compared with the classical ones (full circles), showing a good agreement above E_{tnt}^q/N (vertical dashed line) and a deviation near E_{tnt} (the vertical full line).

probability for the magnetization to reverse its sign. Below the TNT, due to the intrinsic quasi-degeneracy, the dynamics can be entirely characterized by the energy difference δ . This happens when the energy bin ΔE of the initial state is sufficiently small so that one single doublet belongs to it. The dynamics is thus oscillatory with a period given by $2\pi\hbar/\delta$. Indeed under this condition, the magnetization oscillates coherently between states with opposite sign, a phenomenon known as Macroscopic Quantum Coherence[30].

From the results presented here we can address the problem of the dynamical signature of the classical TNT. In the semiclassical limit the crossover region becomes very narrow, ($E_{tnt}^q \rightarrow E_{tnt}$), thus we can expect a crossover from a power law dependence on the energy, like in the classical case[10], to an exponential dependence on the energy. Moreover our previous considerations suggests how the classical limit is recovered: indeed $\delta \approx 0$ as $l \rightarrow \infty$, for energies below E_{tnt} , which is consistent with the fact that the magnetization cannot reverse its sign below E_{tnt} in the classical system.

B. Hard Quantum Regime

The hard quantum regime ($l = 1$), shows many differences with the large l case. In the hard quantum regime we still have doublets and an approximate exponential dependence of δ with the energy, but it is also evident, see Fig. 6, that they change regularly of many order of magnitude in small energy bins.

In order to understand the origin of this regularities, it is useful to rewrite the Hamiltonian(10) as $\hat{H} = \hat{H}_{MF} +$

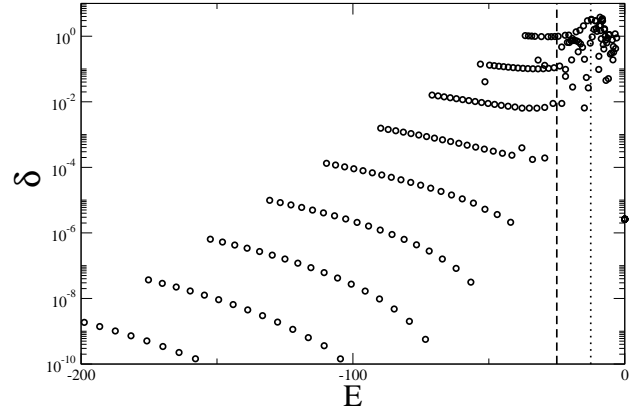


FIG. 6: Splittings δ as a function of the energy per particle, for the case $l = 1$, $N = 50$. Vertical lines are classical non-ergodicity threshold (dotted) and the quantum non-ergodicity threshold (dashed).

\hat{H}_1 , where

$$\hat{H}_{MF} = \frac{\eta}{2} N^2 \hat{m}_x^2 - \frac{1}{2} N^2 \hat{m}_y^2, \quad (13)$$

and

$$\hat{H}_1 = \frac{1}{2} \sum (\hat{S}_i^y)^2 - \frac{\eta}{2} \sum (\hat{S}_i^x)^2. \quad (14)$$

While the mean field part (13) is integrable in the classical limit, the additional term, (14) is responsible for the non integrability of the system. Let us also consider the eigenvectors of \hat{H}_{MF} , $|E_{MF}\rangle$, and expand the eigenvectors of \hat{H} , $|E\rangle$ over them. In other words we consider the probability p_0 that a given eigenvectors of \hat{H} occupies a given eigenvector of \hat{H}_{MF} :

$$p_0 = |\langle E_{MF}|E\rangle|^2.$$

In Fig. 7 we plot for each eigenvalue E of $|E\rangle$ and E_{MF} of $|E_{MF}\rangle$, the relative occupation probability, p_0 . As one can see, the eigenvectors of the full Hamiltonian are almost completely localized on the eigenvectors of the mean field Hamiltonian, see Fig. 7a), over the whole energy range. Actually in the low energy region the eigenvectors occupies just one eigenstate of the mean field Hamiltonian with probability greater the 0.9, while all the other states are occupied with probability smaller the 0.01. The same does not happen in the large l case, see Fig. 7b). Therefore, the non-integrable part (14) is negligible with respect to the mean field (13). The question of the quantum integrability of chaotic Hamiltonians for bosons with $l = 1$ has been recently posed in [31]. Shortly, quantum integrability should be induced, for $l = 1$, by the strong correlations between Hamiltonian matrix elements.

From the above analysis it follows that we can use the mean field Hamiltonian to study the total Hamiltonian in the hard quantum regime. In the next section we will show how to evaluate the eigenvalues of the mean field Hamiltonian for the most part of the spectrum.

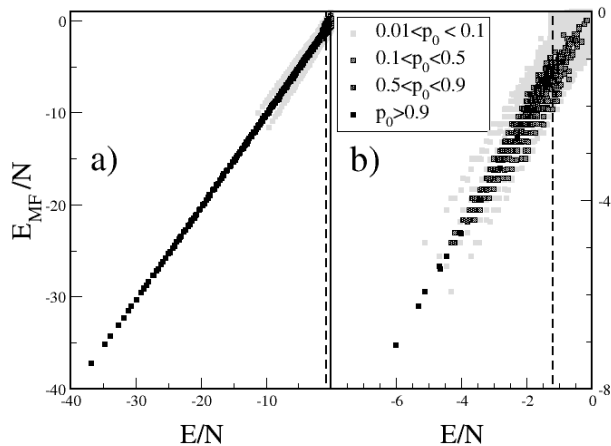


FIG. 7: Probability $p_0 = |\langle E | E_{MF} \rangle|^2$ that an eigenstate $|E\rangle$, with specific energy E/N , occupies an eigenstate $|E_{MF}\rangle$, with specific energy E_{MF}/N . Parameters are : a) $N = 100$, $l = 1$; b) $N = 6$ $l = 4$.

C. High Order Perturbative Approach

Here, we present the results of a high order perturbative calculation of the eigenvalues of the mean field Hamiltonian (13). The Hamiltonian (13) commutes with \hat{m}^2 . The possible values of \hat{m}^2 are given by the possible values of the total magnetic moment which can be obtained combining N particles of spin l , and are determined by the quantum numbers: $Nl, Nl - 1, \dots, 0$. From these values we should exclude those which cannot be combined to give completely symmetric states, if one is interested in the bosonic case (even if the present approach is independent from the statistics). We can thus consider each subspace with different m^2 separately. In this way the many-spin Hamiltonian (14), is equivalent to a set of single spin systems, described by the same Hamiltonian (if we use the rescaled Planck constant, $\hbar = 1/(l(l+1))$), for both) Note that l is the magnitude of the spin of the many-spin problem. Thus in the following we will first consider single spin models, and then we will come back to our many-spin problem.

1. Single Spin Model

In the following we will thus limit our considerations to a single spin of magnitude L , z - component L_z , with $|L_z| \leq L$.

For simplicity we will rewrite the mean field Hamiltonian as follows:

$$\hat{H} = -\hat{m}_z^2 + \eta \hat{m}_x^2 \quad (15)$$

where $|\eta| < 1$ and $\hat{m}_{x,y,z}$ are the components of the total

magnetic moment. Let us notice that Hamiltonian such as $\hat{H} = -J_z \hat{m}_z^2 - J_x \hat{m}_x^2 - J_y \hat{m}_y^2$ can be reduced to (15). The mean-field Hamiltonian (14), can be obtained from (15) after a rotation of π around the x axis which carries y in z and z in $-y$, and does not affect the physics of the problem.

Single-spin-model have an interest in themselves, besides the fact that their analysis will allow us to compute the energy levels of our many-spin mean field Hamiltonian. In recent years growing interest arose in micromagnetic particles [2, 30], such as ferromagnetic domains and magnetic macro-molecules such as Mn_{12} and Fe_8 [32]. The research interest in these systems is mainly due to the possibility to reveal quantum effects in the macroscopic domain, such as the Macroscopic Quantum Tunneling (MQT) of the magnetic moment, and the even more interesting phenomenon of Macroscopic Quantum Coherence (MQC). While in the former case (MQT) the total magnetization of a microscopic particle flip even if classically this would be forbidden by the presence of an effective energy barrier, in the latter case (MQC) the magnetization oscillates between opposite magnetization states in a coherent way. This phenomenon, if revealed, would unambiguously indicate the presence of Quantum Interference of Macroscopic Distinct States [13]. At sufficiently low energy these systems can be modeled by phenomenological single-spin Hamiltonians, where the single spin describes the total magnetic moment of the system. Small magnetic systems described by Single-Spin Hamiltonians with an easy-axis of magnetization where MQT occurs, has been recently investigated experimentally [33, 34]. Splittings of the eigenvalues of the single spin Hamiltonians are simply related to the frequencies of MQC (or the tunneling rates of MQT) [2]. For this reason much effort has been devoted in these years to compute such splittings. Usually, semiclassical methods are employed, such as WKB and imaginary time path integrals to quote but a few [35, 36]. Also perturbation theory can be successfully applied in this kind of problem taking into account high order terms [37]. Indeed it is possible to compute explicitly the first non-zero perturbative contribution to the splittings even if this is an high-order contribution. Here we show that it is possible to estimate the energy threshold at which this approach fails, computing the quantum correction of the TNT.

In Appendix A we show the basic ideas of the high perturbative order approach, and we derive an analytical expression for the eigenvalues and the corresponding splittings (in [37] no explicit derivation was given).

Numerical eigenvalues and their splittings for Hamiltonian (15) and a single spin of magnitude L , have been compared with our results in Fig. 8, where we show the splittings δ as a function of the energy E . In the same figure we can see that while the high perturbative order approach gives a very good estimate for E and δ , in the low energy region of the spectrum, it fails completely in the upper energy region.

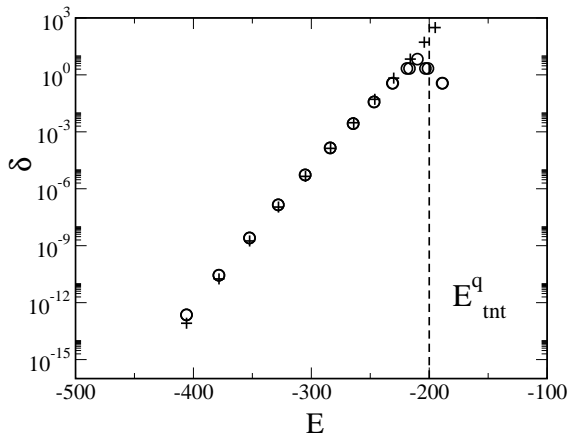


FIG. 8: δ shifts versus the energy E . Eigenvalues and splittings obtained numerically (open circles) and via perturbation theory (crosses) for a single spin $L = 20$. Also shown as vertical dashed line the rough estimates for the validity of our approach. Here is $\hbar = 1$, $\eta = -0.5$.

An upper bound to the energy at which our approach fails can be given evaluating the quantum correction to E_{tnt} for the single spin Hamiltonian, see Eq. (11).

The threshold E_{tnt}^q has been indicated in Fig. 8 as a vertical dashed line, and give a good estimate of the energy at which high order perturbation theory fails.

2. Many spin hamiltonian

We now compare our analytical results with the eigenvalues of the mean field Hamiltonian (14), considered as a many spin hamiltonian and with the eigenvalues of the complete Hamiltonian in the hard quantum regime (10). We can achieve this by considering the possible eigenvalues of \hat{m}^2 , which are obtained when an ensemble of N particles of spin l is considered. Note that from the set of possible eigenvalues of \hat{m}^2 we have to exclude those that are not compatible with the symmetrization postulate (for the bosonic case). For each possible value of \hat{m}^2 we apply our perturbative approach to the correspondent single spin problem. Then, putting all together, we obtain the results for the many-spin Hamiltonian.

In Fig. 9 we plot the splittings versus the specific energy for the mean field Hamiltonian (13) (circles), for the full Hamiltonian (10) (squares), and the perturbative results (crosses). As one can see we can give an accurate good approximation in the low energy region of the spectrum. Deviations obviously appear when the perturbative approach is compared with the splittings of the full Hamiltonian, even if, in this case, the perturbative approach still give a correct order of magnitude estimate of eigenvalues and splitting. From Fig. 9 we can also see how the regular features of δ in the hard quantum regime are related to the quantum numbers of the total angular momentum.

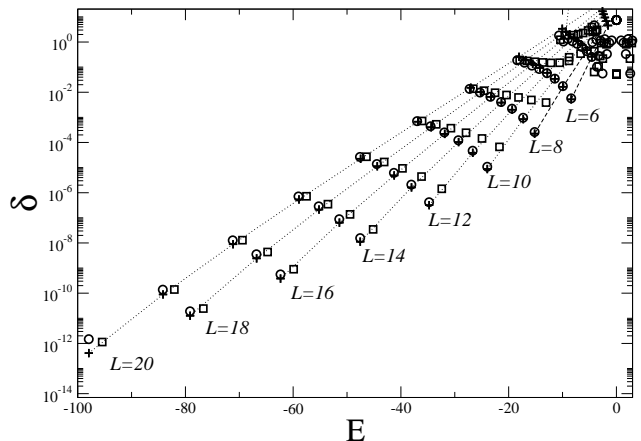


FIG. 9: Energy shifts δ versus E for the many-spin case. Eigenvalues and splittings are compared for the case $N = 20$, $\eta = 1$ and $l = 1$. Circles : mean field approximation; squares : full Hamiltonian; crosses : perturbative result. Eigenvalues are arranged in regular block, according to different L values as indicated in the figure.

One could ask if the same perturbative approach works in the semiclassical regime for the total Hamiltonian (13). Perturbation theory cannot work in the whole energy region, even if we may expect to give an approximate description for low-energy eigenvalues. For instance, applying perturbation theory, e.g. Eq. (A13), for the energy separation between the ground state and the first excited state, we get:

$$\delta_{GS} = \frac{\hbar^2}{4} (1/6)^{Nl}. \quad (16)$$

This expression works fairly well[38], even for large l and it reproduces the main features of the dependence of the ground state splitting, namely the exponential dependence on l , and N as well.

V. CONCLUSIONS

We showed the existence in classical Heisenberg spin models of a Topological Non-connectivity Threshold (TNT), caused by the anisotropy of the coupling when it induces an easy-axis of the magnetization. Below the TNT the constant energy surface is disconnected in two components; in each component the magnetization along the easy axis has a definite sign. Due to the disconnection of the energy surface the magnetization along the easy axis cannot change sign below the TNT inducing a ferromagnetic behavior of the system. Above the TNT, in a strong chaotic regime, the magnetization reverses its sign with an average time diverging as a power law at the TNT. The connection between the TNT and the range of the interaction has also been shown: the existence of this threshold determine a disconnected energy range that remains finite (w.r.t. the total energy range) for long range

interacting macroscopic spin systems while it goes to zero for short range interacting macroscopic spin systems.

On the quantum side the magnetization along the easy axis can change its sign also below the TNT through Macroscopic Quantum Tunneling. This leads to the the problem of defining a quantum signature of the classical TNT. We have found a quantum signature of the classical TNT in the spectral properties of the system leading to the definition of a quantum disconnection threshold, E_{tnt}^q , with the correct classical limit. Below E_{tnt}^q the spectrum is characterized by the presence of quasi degenerate doublets, whose energy difference increases exponentially with the energy only up to E_{tnt}^q . The quantum reversal times of the total magnetization have been studied and compared with the classical ones above the TNT. Thus this threshold indicates an energy range (which is not negligible w.r.t. the total energy range for long range interacting systems) in which Macroscopic Quantum Phenomena can be studied.

APPENDIX A: HIGH ORDER PERTURBATIVE APPROACH

In this section we present the results of a high perturbative order calculation of the eigenvalues of the single spin Hamiltonian (15). We will show that in order to split the double degenerate levels of the $-\hat{m}_z^2$ term of (15) characterized by the quantum number $l_0 = |m_z|$, the first non-zero contribution is at the l_0 -th perturbative order. This also give a qualitative explanation of the well known exponential dependence of the splitting magnitudes on the energy.

Let us consider a single spin of magnitude L , z -component L_z with $|L_z| \leq L$ and $|L, L_z\rangle$ as basis states.

Hamiltonian (15) can be written as $\hat{H} = \hat{H}_0 + \hat{V}$, where :

$$\begin{aligned}\hat{H}_0 &= -\hat{m}_z^2 + \frac{1}{4}\eta(\hat{m}^+\hat{m}^- + \hat{m}^-\hat{m}^+) \\ \hat{V} &= \frac{1}{4}\eta(\hat{m}^+\hat{m}^+ + \hat{m}^-\hat{m}^-)\end{aligned}\quad (\text{A1})$$

and

$$\hat{m}^\pm |L, L_z\rangle = \sqrt{L(L+1) - L_z(L_z \pm 1)} |L, L_z \pm 1\rangle. \quad (\text{A2})$$

Since \hat{H}_0 is diagonal in the basis $|L, L_z\rangle$, the unperturbed energy $E_0 = \langle L, l_0 | \hat{H} | L, l_0 \rangle$ are given by:

$$E_0(L, l_0) = -\hbar^2 l_0^2 + \frac{1}{2}\hbar^2 \eta [L(L+1) - l_0^2] \quad (\text{A3})$$

Each unperturbed energy level turns out to be doubly degenerate, with eigensubspaces spanned by $|L, \pm l_0\rangle$. The first non-zero contribution to the splitting of a degenerate pair occurs at the l_0 -th order of perturbation

theory. In order to show that let us define the n -th order perturbation operator [39]:

$$\hat{\mathcal{P}}^{(n)} = \hat{V} \left(\frac{\hat{\phi}}{E_0 - H_0} \hat{V} \right)^{n-1}, \quad (\text{A4})$$

where $\hat{\phi} = 1 - \sum_{E'_0 \neq E_0} |E'_0\rangle \langle E'_0|$ is the projector out of the considered degenerate subspace. The right linear combination of the unperturbed basis vectors $|L, \pm l_0\rangle$ (to which eigenstates of \hat{H} tend when \hat{V} is negligible) can be found by diagonalizing the following matrix:

$$\begin{pmatrix} \mathcal{P}_{++}^{(n)} & \mathcal{P}_{+-}^{(n)} \\ \mathcal{P}_{-+}^{(n)} & \mathcal{P}_{--}^{(n)} \end{pmatrix} \quad (\text{A5})$$

where $\mathcal{P}_{ss'}^{(n)} = \langle L, sl_0 | \hat{\mathcal{P}}^{(n)} | L, s'l_0 \rangle$, $s, s' = \pm 1$ and n is the minimum order giving rise to two different eigenvalues of the matrix (A5). A π -rotation around the x -axis leaves \hat{V} unchanged since $|L, l_0\rangle \rightarrow |L, -l_0\rangle$, and $\hat{m}^\pm \rightarrow \hat{m}^\mp$. Then $\mathcal{P}_{++}^{(n)} = \mathcal{P}_{--}^{(n)}$, $\mathcal{P}_{+-}^{(n)} = \mathcal{P}_{-+}^{(n)}$ and the right combination of unperturbed basis vectors is:

$$|\pm m_0\rangle = \frac{1}{\sqrt{2}}(|L, l_0\rangle \pm |L, -l_0\rangle). \quad (\text{A6})$$

Eigenvalues undergo a shift given by $\pm \mathcal{P}_{+-}^{(n)}$. The generic n -th order energy shift, $\Delta^{(n)}$ induced by the perturbation is given by:

$$\Delta^{(n)} = \langle \pm m_0 | \hat{\mathcal{P}}^{(n)} | \pm m_0 \rangle \quad (\text{A7})$$

While the degeneracy can be removed only by non-zero off-diagonal elements, an overall energy shift D can be induced by non-zero diagonal elements too.

In order to compute D and δ the action of $\hat{\mathcal{P}}^{(n)}$ on the basis states $|L, \pm l_0\rangle$ should be evaluated. If $n = 1$ then $\hat{\mathcal{P}}^{(1)} = \hat{V}$. In this case the diagonal elements of the matrix (A5) are zero since \hat{V} can only change $l_0 \rightarrow l_0 \pm 2$. Off-diagonal elements $\langle L, -l_0 | \hat{V} | L, +l_0 \rangle$ are different from zero only when \hat{V} brings $|L, l_0\rangle$ into $|L, -l_0\rangle$. This can happen only if $l_0 = 1$.

If $n = 2$ then $\hat{\mathcal{P}}^{(2)} = \hat{V}(\hat{\phi}/(E_0 - H_0))\hat{V}$. Since

$$\frac{\hat{\phi}}{(E_0 - H_0)} |L, l\rangle = \frac{1 - \delta_{l, l_0}}{E_0(L, l_0) - E_0(L, l)} |L, l\rangle \quad (\text{A8})$$

in order to understand the action of $\hat{\mathcal{P}}^{(2)}$ we have to apply \hat{V} twice. Let's consider the diagonal elements: Can we take $|L, l_0\rangle$ in itself $|L, l_0\rangle$, using \hat{V} twice? Yes: $\hat{V}\hat{V}|L, l_0\rangle \rightarrow \hat{V}(|L, l_0 - 2\rangle + |L, l_0 + 2\rangle) \rightarrow |L, l_0\rangle + |L, l_0 - 4\rangle + |L, l_0 + 4\rangle + |L, l_0\rangle$, where the coefficients in front of the states have been omitted. Bracketing the final states thus obtained with $|L, l_0\rangle$, only the first and the last remain. Then there are two "ways" in which the operator

$\hat{\mathcal{P}}^{(2)}$ can take $|L, l_0\rangle$ in itself: if $l_0 > 1$ by the following chain rule : $|L, l_0\rangle \rightarrow |L, l_0 - 2\rangle \rightarrow |L, l_0\rangle$, while if $l_0 < L - 1$ by $|L, l_0\rangle \rightarrow |L, l_0 + 2\rangle \rightarrow |L, l_0\rangle$.

It is now easy to compute the first non zero contributions to the overall shift. From (A7) we have:

$$D = \langle L, \pm l_0 | \hat{V} \left(\frac{\hat{\phi}}{E_0 - H_0} \hat{V} \right) | L, \pm l_0 \rangle, \quad (\text{A9})$$

The contributions $D_{1,2}$ coming from the two ways described above, are:

$$D_1 = \begin{cases} \left(\frac{\eta \hbar}{4} \right)^2 \frac{f^-(L, l_0) f^-(L, l_0 - 1)}{\Delta E_0^-} & \text{for } l_0 > 1 \\ 0 & \text{for } l_0 \leq 1 \end{cases} \quad (\text{A10})$$

and

$$D_2 = \begin{cases} \left(\frac{\eta \hbar}{4} \right)^2 \frac{f^+(L, l_0) f^+(L, l_0 + 1)}{\Delta E_0^+} & \text{for } l_0 < L - 1 \\ 0 & \text{for } l_0 \geq L - 1 \end{cases} \quad (\text{A11})$$

where $f^\pm(L, l_0) = L(L + 1) - l_0(l_0 \pm 1)$ and $\Delta E_0^\pm =$

$E_0(L, l_0) - E_0(L, l_0 \pm 2)$. Thus, $D = D_1 + D_2$ is the first non-zero overall energy shift.

Let us now consider the off-diagonal matrix elements. It is possible to go from $|L, l_0\rangle$ to $|L, -l_0\rangle$ using \hat{V} twice only when $l_0 = 2$. In this case there is one only way: $|L, l_0\rangle \rightarrow |L, l_0 - 2\rangle \rightarrow |L, l_0 - 4\rangle = |L, -l_0\rangle$, the last being true only for $l_0 = 2$. It is then clear why the first non-zero operator which splits the doublet characterized by L, l_0 is the l_0 -th order. From (A7) we have:

$$\delta = 2 \langle L, l_0 | \hat{V} \left(\frac{\hat{\phi}}{E_0 - H_0} \hat{V} \right)^{l_0-1} | L, -l_0 \rangle \quad (\text{A12})$$

From Eq.(A12) there is only one way to connect $|L, l_0\rangle$ with $|L, -l_0\rangle$, namely $|L, l_0\rangle \rightarrow |L, l_0 - 2\rangle \dots \rightarrow |L, -l_0 + 2\rangle \rightarrow |L, -l_0\rangle$. After some algebra, one has:

$$\delta = \hbar^2 \left(\frac{\eta}{4} \right)^{l_0} (-1)^{l_0-1} \frac{\prod_{j=-l_0}^{l_0-1} \sqrt{L(L+1) - j(j+1)}}{\prod_{p=1}^{l_0-1} (4 + 2\eta)p(l_0 - p)} \quad (\text{A13})$$

To summarize, for any given degenerate doublet we can calculate the overall shift D , Eqs.(A10,A11) and the splitting δ , Eq.(A13).

-
- [1] F. Borgonovi, G. L. Celardo, M. Maianti, E. Pedersoli, J. Stat. Phys., **116**, 516 (2004).
- [2] E. M. Chudnovsky and J. Tejada, *Macroscopic Quantum Tunneling of the Magnetic Moment*, Cambridge University Press, (1998).
- [3] M. Hartmann, G. Mahler and O. Wess. Phys. Rev. Lett. **93**, 80402 (2004).
- [4] J. Barré, D. Mukamel, S. Ruffo, Phys. Rev. Lett. **87**, 3, (2001).
- [5] J. Barré, F. Bouchet, T. Dauxois, and S. Ruffo, Phys. Rev. Lett. **89**, 110601, (2002)
- [6] R. G. Palmer, Adv. in Phys., **31**, 669 (1982).
- [7] A. I. Khinchin *Mathematical Foundations of Statistical Mechanics*, Dover Publications, New York (1949).
- [8] L.Caiani, L.Casetti, C.Clementi, M.Pettini, Phys. Rev. Lett. **79**, 4361 (1997); L.Casetti, M.Pettini, E.G.D.Cohen, Phys. Rept. **337**, 237 (2000); L.Casetti, M.Pettini, E.G.D.Cohen, J.Stat.Phys. **111**, 1091 (2003).
- [9] F. Borgonovi, G.L. Celardo, A. Musesti, and R. Trasarti-Battistoni cond-mat/0505209.
- [10] G.L.Celardo, J.Barré, F.Borgonovi, S. Ruffo, cond-mat/04010119.
- [11] T. Dauxois, S. Ruffo, E. Arimondo, M. Wilkens Eds.,Lect. Notes in Phys., **602**, Springer (2002).
- [12] F. Borgonovi, G. L. Celardo, and G. P. Berman, cond-mat/0506233.
- [13] A. J. Leggett and A. Garg, Phys. Rev. Lett. **54**, 857 (1985), A. J. Leggett, J. Phys., **14**, R415-R451 (2002), A. J. Leggett, Rev. Mod. Phys. **59**, 1, (1987).
- [14] P. Bruno, Phys. Rev. B, **39**, 865 (1989).
- [15] G. van der Laan, J. Phys. : Consens. Matter **10**, 3239 1998.
- [16] U. Gradmann Handbook of Magnetic Materials, vol 7, ed. K. H. Buschow (Amsterdam : Elsevier) pp 1-96 (1993).
- [17] M. Tischer, O. Hjortstam, D. Arvanitis, J. H. Dunn, F. May, K. Baberschke, J. Trygg and J. Wills, Phys. Rev. Lett. **75**, 102 (1995).
- [18] D. Weller, J. Stohr, R. Nakajima, A. Carl, M. G. Samant, C. Chappert, R. Megy, P. Beauvillain, P. Veillet and G. Held, Phys. Rev. Lett. **75** 3752 (1995).
- [19] P. Ohresser, G. Ghirindelli, O. Tjernberg and N. Brookes, Phys. Rev. B **62**, 5803 (2000).
- [20] P. Gambardella, S. Dhesi, S. Gardonio, C. Grazioli, P. Ohresser and C. Carbone, Phys. Rev. Lett. **88**, 47202 (2002).
- [21] I. M. L. Billas, A. Chatelain and W. A. de Heer. Science **265**, 1682 (1994).
- [22] H. A. Durr, S. Dhesi, E. Duzdik, D. Knabben, G. van der Laan, J. B. Goedkopp and F. U. Hillebrecht, Phys. Rev. B **59**, R701 (1999).
- [23] J. Dorantes-Davila and G. M. Pastor, phys. Rev. Lett. bf **81**, 208 (1998).
- [24] B. Lazarovits, L. Szunyogh and P. Weinberger, Phys. Rev. B **67**, 024415 (2003).
- [25] J. Hong and R. Wu, Phys. Rev. B **67**, 20406R (2003).
- [26] R. M. White, *Quantum Theory of Magnetism*, McGraw-Hill Book Company, New York (1970).
- [27] B. V. Chirikov Phys. Rep., **52**, 253 (1979).
- [28] J. Ford, , Phys. Rep. **213**, 271 (1992).
- [29] G. P. Berman and F. M. Izrailev, Chaos **15**, 015104

- (2005).
- [30] S.Takagi, *Macroscopic Quantum Tunneling*, Cambridge University Press, (1997).
- [31] L. Benet, T. Rupp and H. A. Weidenmuller, Phys. Rev. Lett. **87**, 010601 (2001); T. Asaga, L. Benet, T. Rupp and H. A. Weidenmuller, Europhys. Lett. **56**, 340 (2001); T. Asaga, L. Benet, T. Rupp and H. A. Weidenmuller, Ann. of Phys. **298** 229 (2002).
- [32] J. Schnack, cond-mat/0501625.
- [33] W. Wernsdorfer and R. Sessoli, Science **284**, 133, (1999).
- [34] L. Thomas et al, Nature **383**, 145, (1996).
- [35] M.Enz and R.Schilling, J.Phys. C, **19**, 1765-1770 (1986), M.Enz and R.Schilling, J.Phys. C, **19**, L711-L715 (1986), G.Scharf, W.F.Wreszinski and J.L.Hemmen, J.Phys. A, **20**, 4309-4319 (1987).
- [36] E.M.Chudnovsky and L. Gunther, Phys. Rev. Lett. **60**, 611 (1988).
- [37] D.A. Garanin, J. Phys. A **24**, L61-L62 (1991).
- [38] G. L. Celardo, PhD dissertation , University of Milan, Italy (2004).
- [39] J.J. Sakurai, *Modern Quantum Mechanics*, Addison-Wesley Publishing Company (1985).